Nov 7th, 12:00 AM - Nov 8th, 12:00 AM

The Impact of Bearing Conditions on the Behavior of Cold-Formed Steel Stud Assemblies

Abbas Joorabchian

Zhanjie Li

Kara D. Peterman

Wei-Wen Yu International Specialty Conference on Cold-Formed Steel Structures
St. Louis, Missouri, U.S.A., November 7 & 8, 2018

The impact of bearing conditions on the behavior of cold-formed steel stud assemblies

Abbas Joorabchian[1], Zhanjie Li[2], Kara D. Peterman[3]

Abstract

The objective of this study is to explore the structural response of cold-formed steel stud assemblies (i.e., stud and track) with partial bearing conditions. It is hypothesized that studs bearing under partial bearing conditions (i.e., not fully bearing on a concrete slab) may result in reduced axial capacities. Currently, the behavior of these systems on concrete slabs due to member instabilities is not well-understood, and cold-formed steel design specifications provide no guidance. This study provides an integral experimental and numerical investigation of the stability response of the studs under partial bearing conditions in order to quantify the reduction of their axial capacities. A variety of partial bearing conditions are considered in this study by parametrically varying edge (i.e., where the steel stud assembly is close to the concrete slab edge) and overhang (i.e., steel stud assembly is outside the edge) distances. The non-uniform bearing stress underneath the stud caused by concrete cracking, crushing, or a combination thereof is measured to relate with the reduction of the axial capacity of the stud. The results of this study will be used to develop design guidelines for stud wall assembly under non-uniform bearing conditions.

[1,3] Department of Civil and Environmental Engineering, University of Massachusetts Amherst, MA, USA
[2] Department of Engineering, The SUNY Polytechnic Institute, Utica, NY, USA

1. Introduction

Light framed construction is utilizing cold-formed steel (CFS) members widely for both structural (load bearing) and nonstructural members. CFS studs which generally form the walls of such buildings are commonly capped in horizontal tracks at the top and bottom (Figure 1)[1,2]. The walls are typically placed on the concrete slab floors, at some distance from the slab edge (or indeed overhanging from the slab). This is especially true for exterior walls and result in a non-uniform bearing condition for the studs leading to a non-uniform stress distribution on the stud end. Studs bearing under these situations will have reduced axial capacity, and current practice does not currently recognize a difference in axial capacity or behavior due to partial end supports; AISI standards AISI S100-16 and S240-15 do not provide guidance on the calculation of this reduced axial capacity [3,4].

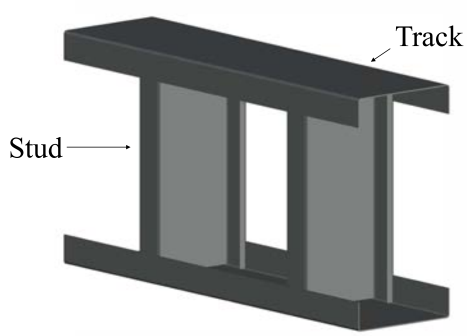

Figure 1: Stud-track assemblies

A wealth of data exists on the performance of axially-compressed studs and stud assemblies, but in previous work, the concrete slabs are assumed to provide rigid uniform support resulting in a uniform stress distribution on the stud end [1,2], [5–11]. These works further do not capture the spalling or crushing of the concrete slab, which only intensifies the non-uniform condition at the stud end and may ultimately reduce contact.

Bae, et at [12] investigated the axial strength of CFS walls on concrete slabs. The research program was experimental in nature, and primarily examined the effect of wall stud configurations on the performance of the system. Single stud columns, single stud walls, back-to-back stud columns, and back-to-back stud walls were tested on an 89mm concrete slab intended to simulate typical residential floor systems. Specimens were cut to 51 mm in height to force failure into the slab, rather than buckling of the stud. FEM was conducted to determine the stress distribution in the concrete slab, through the track section. The work demonstrated that edge distance did impact system bearing strength, and results were used to develop a method of determining the bearing area for the stud-track assembly on concrete slabs, which accurately predicted experimental results. It also demonstrated the inadequacy and inapplicability of the bearing provisions in ACI 318-05 (Building Code Requirements for Reinforced Concrete) for CFS wall systems. While this study expanded the state of knowledge for how stud assemblies interact with concrete foundations, it was limited in scope to one stud size and one stud height which in turn restricted failure modes to the slab and did not permit local buckling of the stud. Research from the University of Manitoba [13] also supports a reduction in stud axial capacity due to stud distance from slab edge. The experimental program undertaken by the authors included stud assemblies located 8" from the stud edge, and assemblies located at the stud edge. The studs were sized such that they were permitted to buckle locally, unlike in the Bae et al [12] work. Assemblies located at 8" from the slab edge developed their local buckling capacity while those installed on the edge were hindered by concrete spalling and cracking – their axial compressive strength decreased by 15-25%, due to the reduction in bearing area, and loss of a uniform stress distribution. The work examined one stud-track assembly and did not consider intermediate edge distances. Neither of these studies explore a range of studs and track assemblies.

The aim of this research project is to quantify the impact of the concrete slab as a flexible or semi-rigid support and the edge distance on the axial capacity of stud-track assemblies. This paper starts with describing the statement of the work and then an explanation about the computational finite element model. Results and a brief description of experimental test follow.

3. Statement of work

This paper is a part of a comprehensive research project the aim of which is to characterize experimentally and computationally the effect of stud bearing on Concrete, examining overhang distance, edge distance, and various assembly configurations. Table 1 demonstrates which specimen configuration are to be included in the experimental test matrix. All configurations will be modeled in ABAQUS [14], to validate the experimental results. It should be noted that the Phase 1 is not included in Table 1 and it is for the rigid bearing condition.

Table 1: Experimental and computational test matrix

Stud	Phase 2: Full Bearing Condition	Phase 3: Edge Condition	Phase 4: Effect of Overhange
600S162-33	Full bearing (edge distance>6 ")	at slab edge 1" from slab edge 0.5" from slab edge 0.125" from slab edge	0.5" overhang 1" overhang
600S162-54	Full bearing (edge distance>6 ")	at slab edge 1" from slab edge 0.5" from slab edge 0.125" from slab edge	0.5" overhang 1" overhang
600S162-97	Full bearing (edge distance>6 ")	at slab edge 1" from slab edge 0.5" from slab edge 0.125" from slab edge	0.5" overhang 1" overhang

Stud	Phase 5: Effect of Flange Width
600S300-33	at slab edge 1" from slab edge 0.5" from slab edge
600S300-97	at slab edge 1" from slab edge 0.5" from slab edge

This paper focusses on the finite element model and the computational result of stud 600S162-54 in rigid bearing, full bearing, 1 inch (25.4 mm) from slab edge, and at slab edge.

4. Geometry and finite element model

The system consists of two 600S162-54 CFS members of 12 inches (30.48 mm) which are spaced 12 inches (30.48 mm) and two 24 inches (60.96 mm) 600T125-54 tracks. For the conditions including reinforced concrete slab, a slab of 34x22x6 inches (86.36x55.88x15.24 cm) is considered. In order to reinforce the concrete slabs, two layers of 6x6 W4 welded mesh are utilized.

For this project, the finite element modeling is done in ABAQUS [14]. For the stud-track assembly a total of 9166 S46 shell elements and for the reinforced concrete a total of 1380 C3D8R hexahedral solid and 2480 T3D2 truss elements are used. The stud to track fasteners and track to concrete fasteners are simulated by linear multi-point constraint. The interaction between stud and track flanges are simulated as a surface to surface contact and penalty friction coefficient equal to 0.2 is considered. For the steel to concrete interaction, the friction coefficient is considered 0.5. The contact between track and stud webs are simulated by tie constraint. The meshes are embedded into the concrete slab and they are constrained to the slab by embedded region constraint.

For simulating the boundary conditions, for the model with rigid support (no concrete slab), the web of the bottom track is constrained in three transitional degrees of freedom. In addition, the web of the top track is constrained in two in-plane transitional degree of freedom. For the models with slab, instead of the bottom track, the bottom of the concrete slab is constrained. In Figure 2, the finite element model for 1 inch (24 mm) edge condition is illustrated.

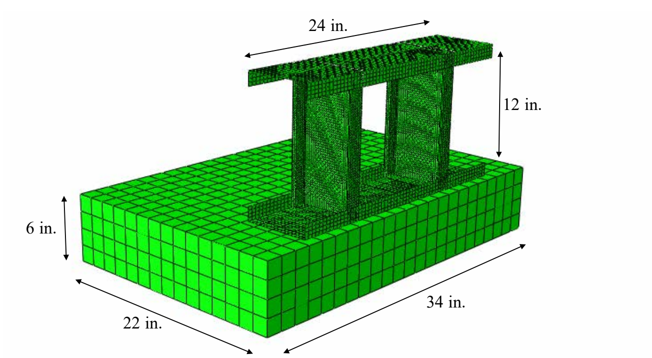

Figure 2: Finite element model of stud-track assembly placed on top of a concrete slab with 1 inch edge distance; the studs are 600S162-54 and the tracks are 600T125-54

5. Computational analysis of one of the configurations and its results

This section includes nonlinear static analysis of perfect and imperfect models.

5.1. Nonlinear static analysis of perfect models

In this section, nonlinear static analysis for the perfect model is performed in ABAQUS to compare the strength and stiffness of stud-track assembly under different conditions. A displace-control load is applied on the top track to simulate the behavior of actuator in the experimental tests. The displacement rate is considered 0.01 in/sec (0.254 mm/sec) and the maximum displacement is set 0.1 inch (2.54 mm). The deformed shapes of the model with rigid bearing support and the model with one inch distance to the edge under the peak loads are shown in the Figure 3. In Figure 4 load versus displacement curves of the perfect finite element models are plotted.

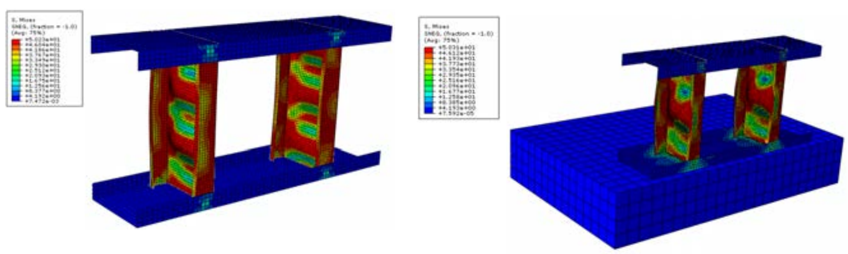

(a) (b)

Figure 3: 3D view of deformed stud-track assembly under the peak loads; (a) rigid bearing condition, (b) 1 inch edge distance condition

As it can be seen in Figure 4, the model with rigid bearing support has the maximum capacity and the reverse for the model located at the slab edge. Due to the rigid support, the stress distribution is uniform at stud end while a non-uniform support causes a non-uniform stress distribution which may decrease the capacity of the system. In full bearing condition, because the stud-track assembly is installed on the slab center, the slab can almost act as a rigid support and maintain a uniform stress distribution. However, as shown in Figure 4 and Table 2, decreasing edge distance can dramatically impact axial capacity and stiffness.

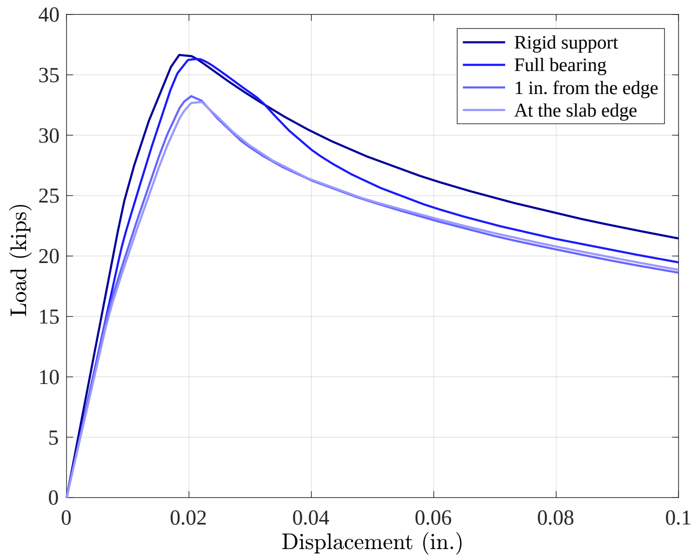

Figure 4: Load-displacement plots of perfect models

Table 2: Results summary of the perfect models

System	Peak load (kips)	Difference in Peak load (%)	Stiffness (kips/in)	Difference in peak load (%)
Rigid bearing	36.55	-	2632	-
Full bearing	36.30	0.68	2306	0.68
1 in. to the edge	33.23	9.08	2278	9.08
At the edge	32.75	10.40	2204	10.40

5.2. Nonlinear static analysis of imperfect models

CFS members are not perfect and they may have inherent imperfections from the manufacturing, shipping, and construction process. The imperfection can affect the behavior of a structure and this has been well-documented by other researchers. Therefore, the models sensitiveness to the imperfection is explored in this section.

Eigenmodes of elastic buckling analysis are utilized to apply geometric imperfections to the models and the imperfections are defined in mode shapes forms for stud-track assembly. The amplitude of imperfection is considered one-tenth of the stud thickness. Non-linear static analysis is performed for the imperfect models and the force-displacement curves are plotted in Figure 5.

As Figure 5 and Table 3 demonstrate, the imperfection may affect the strength of the stud-track assembly when there is a rigid bearing or full one. However, the impact of imperfection on the systems located near the edge or at the edge is not significant and they are not imperfection sensitive. Table 3 indicates when the imperfection is defined, the peak loads of models are almost same though the model with rigid bearing support still has the largest axial capacity. As the stud-track assembly get closer to the edge, the impact of imperfection is more negligible. This change in behavior with the inclusion of imperfections may reflect the progression of failure in the stud assembly-slab systems. In perfect systems, load is distributed to the slab prior to instability, whereas in imperfect systems, the studs buckle prior to this load distribution. While the rigid and full bearing conditions have ~8% reduction in peak axial capacity with the introduction of imperfections, the same reductions are less than 1% for the small edge distance specimens. Thus, the impact of bearing at or near the slab edge is lessened due to the progression of failure in imperfect models.

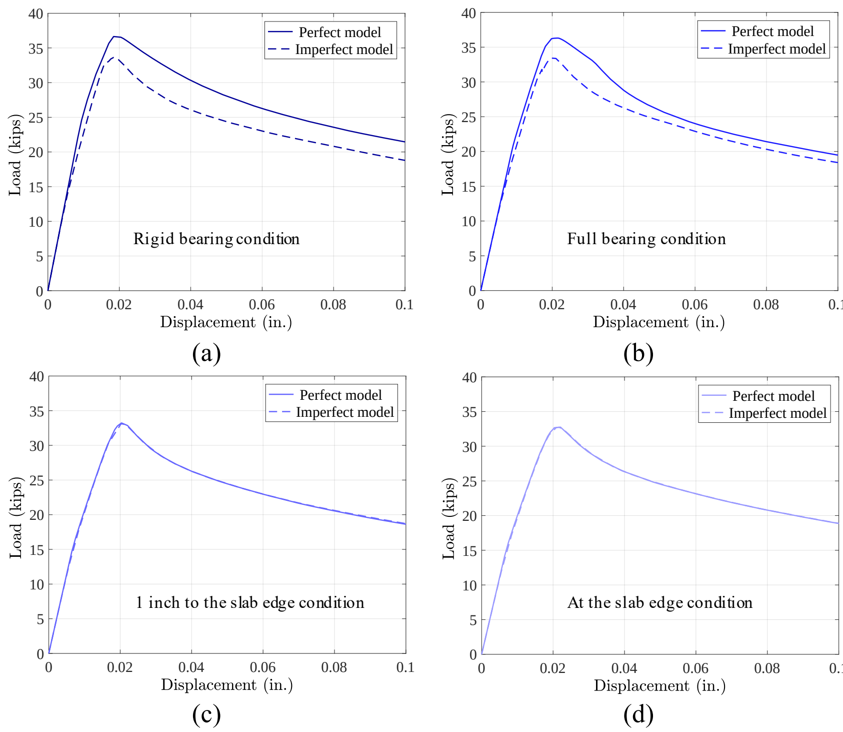

Figure 5: Comparison between the behavior of perfect and imperfect models; (a) rigid bearing condition, (b) full bearing condition, (c) 1 inch to the slab edge condition, (d) at the slab edge condition

Table 3: Comparison between the peak load of perfect and imperfect assembly

System	Peak load in perfect models (kips)	Peak load in imperfect models (kips)	Difference (%)
Rigid bearing	36.55	33.62	8.02
Full bearing	36.30	33.42	7.93
1 in. to the edge	33.23	33.11	0.36
At the edge	32.75	32.73	0.06

6. Future work

The experimental testing provides numerous benefits in verification and validation for the nonlinear finite element models and reliable strength predictions for the developments of design provisions. A test rig and a 110 kips (490 KN) actuator at University of Massachusetts, Amherst structural lab are utilized. The load will be applied to short beam designed to distribute the load from the actuator to the top track of stud assemblies. In order to provide a rigid support, a rigid I-beam is designed to be placed underneath of stud-track assemblies. For non-rigid bearing support conditions, the assemblies will bear directly on the 34x22x6 inches (86.36x55.88x15.24 cm) slabs. Powder-actuated fasteners will be utilized to connect assemblies to slabs. Table 1 demonstrates which specimen configurations are to be included in the experimental test matrix. A schematic view of the experimental test is shown in Figure 6.

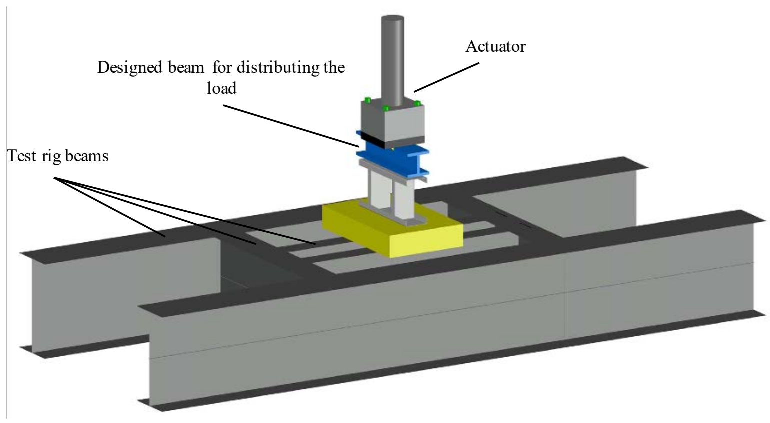

Figure 6: The schematic view of experiment tests

This work is planned in the coming months and will validate results from computational modeling. Furthermore, the modeling campaign will be expanded to fully encapsulate the experimental test matrix. After the experimental results are fully validated, parametric studies will be conducted with experimental variables not able to be tested.

Conclusion

The impact of non-uniform and partial bearing conditions are explored on axial capacities of stud-bearing assemblies. According to the distance of the assembly to the edge, non-uniform bearing support can play a more significant role. For the perfect assembly consisting of two 600S162-54 capped in two horizontals 600T125-54, the full bearing condition almost does not affect the axial capacity; however, when the assembly is located in 1 inch to the edge or at the concrete slab edge, the axial capacity decreased 9.08% and 10.40% respectively. The imperfection sensitiveness of assemblies is explored as well. The results demonstrate that the imperfection does not affect the axial capacity of the assemblies at the edge or 1 inch to the edge while it decreases the peak load of models with rigid and non-uniform bearing support 8.02% and 7.93% respectively. As a result, due to the impact of partial bearing conditions on the capacity of stud-track assemblies, it is recommended their impact be considered in CFS stud wall assemblies behavior.

Acknowledgement

The authors would like to gratefully thank American Iron and Steel Institute (AISI) for their financial support, Super Stud Building Products for donation of studs and tracks and Hilti for donation of fasteners and fasteners gun and Mark Gauthier, the University of Massachusetts Amherst lab technician for his help.

References

[1] K. D. Peterman, B. W. Schafer, "Sheated cold-formed steel studs under axial and lateral load," J. Constr. Steel Res., vol. 140, no. 10, pp. 1–12, 2014.

[2] L. C. M. Vieira, Y. Shifferaw, and B. W. Schafer, "Experiments on sheathed cold-formed steel studs in compression," J. Constr. Steel Res., vol. 67, no. 10, pp. 1554–1566, 2011.

[3] AISI S100, North America Specification for the Desighn of Cold- Formed Steel Structures, American Iron and Steel Institude, Washington, D.C., 2016.

[4] AISI S240, North America Standard for Cold-Formed Steel Structural Framing, American Iron and Steel Institude, Washington, D.C., 2015.

[5] L. C. M. Vieira and B. W. Schafer, "Behavior and Design of Sheathed Cold-Formed Steel Stud Walls under Compression (Ph.D. Thesis), The John Hopkins University, 2011.

[6] I. Georgieva, L. Schueremans, and L. Pyl, "Composed columns from cold-formed steel Z-profiles: Experiments and code-based predictions of the overall compression capacity," Eng. Struct., vol. 37, pp. 125–134, 2012.

[7] Y. Li, Y. Li, S. Wang, and Z. Shen, "Ultimate load-carrying capacity of cold-formed thin-walled columns with built-up box and i section under axial compression," Thin-Walled Struct., vol. 79, pp. 202–217, 2014.

[8] J. Ye, R. Feng, W. Chen, and W. Liu, "Behavior of cold-formed steel wall stud with sheathing subjected to compression," J. Constr. Steel Res., vol. 116, pp. 79–91, 2016.

[9] X. Liu and T. Zhou, "Research on axial compression behavior of cold-formed triple-lambs built-up open T-section columns," J. Constr. Steel Res., vol. 134, pp. 102–113, 2017.

[10] F. Liao, H. Wu, R. Wang, and T. Zhou, "Compression test and analysis of multi-limbs built-up cold-formed steel stub columns," J. Constr. Steel Res., vol. 128, pp. 405–415, 2017.

[11] D. C. Fratamico, S. Torabian, K. J. R. Rasmussen, and B. W. Schafer, "Experimental studies on the composite action in wood-sheathed and screw-fastened built-up cold-formed steel columns," Struct. Stab. Res. Counc. Annu. Stab. Conf. 2016, SSRC 2016, vol. 127, no. January, pp. 290–305, 2016.

[12] S. Bae, A. Belarbi, and R. A. LaBoube, "Bearing Strength of Slabs on Grade Supporting a Cold-Formed Steel Wall in Low-Rise Building," J. Archit. Eng., vol. 12, no. 1, pp. 24–32, 2006.

[13] D. Polyzois, S. Fox, "Bearing of Steel Studs on Concrete," Newsletter for the Light Gauge Steel Engineering Association (now the Cold-Formed Steel Engineering Institute), 2011

[14] Abaqus 6.14-4. Simulia, Dassault Systems, Providence, RI, 2014.